EPJ manuscript No.
(will be inserted by the editor)

Revisiting the scaling of the specific heat of the three-dimensional random-field Ising model

Nikolaos G. Fytas[1], Panagiotis E. Theodorakis[2], and Alexander K. Hartmann[3]

[1] Applied Mathematics Research Centre, Coventry University, Coventry CV1 5FB, United Kingdom
[2] Institute of Physics, Polish Academy of Sciences, Al. Lotników 32/46, 02-668, Warsaw, Poland
[3] Institut für Physik, Universität Oldenburg, Carl-von-Ossietzky-Straße 9-11, 26111 Oldenburg, Germany

Received: date / Revised version: date

Abstract. We revisit the scaling behavior of the specific heat of the three-dimensional random-field Ising model with a Gaussian distribution of the disorder. Exact ground states of the model are obtained using graph-theoretical algorithms for different strengths h of the random fields and system sizes containing up to $\mathcal{N} = 268^3$ spins. By numerically differentiating the bond energy with respect to h, a specific-heat-like quantity is obtained whose maximum is found to converge to a constant at the thermodynamic limit. Compared to a previous study following the same approach, we have studied here much larger system sizes with an increased statistical accuracy. We discuss the relevance of our results under the prism of a modified Rushbrooke inequality for the case of a saturating specific heat. Finally, as a byproduct of our analysis, we provide high-accuracy estimates of the critical field $h_c = 2.279(7)$ and the critical exponent of the correlation exponent $\nu = 1.37(1)$, in excellent agreement to the most recent computations in the literature.

PACS. PACS. 05.50+q Lattice theory and statistics (Ising, Potts. etc.) – 64.60.De Statistical mechanics of model systems – 75.10.Hk Classical spin models – 75.10.Nr Spin-glass and other random models

1 Introduction

The random-field Ising model (RFIM) is one of the archetypal disordered systems [1–11], extensively studied due to its theoretical interest, as well as its close connection to experiments in hard [12–15] and soft condensed matter systems [16]. Its beauty is that the mixture of random fields and the standard Ising model creates rich physics and leaves many still unanswered problems. The Hamiltonian describing the model is

$$\mathcal{H} = -J \sum_{<i,j>} \sigma_i \sigma_j - \sum_i h_i \sigma_i, \qquad (1)$$

where $\sigma_i = \pm 1$ are $\mathcal{N}$ Ising spins, $J > 0$ is the nearest-neighbor's ferromagnetic interaction, and h_i are independent quenched random fields. Several field distributions have been considered in the literature, the most common ones being the Gaussian and bimodal distributions [14, 17–19].

The existence of an ordered ferromagnetic phase for the RFIM, at low temperature and weak disorder, followed from the seminal discussion of Imry and Ma [1], when the spatial dimension $D > 2$ [17–21]. This has provided us with a general qualitative agreement on the sketch of the phase boundary, separating the ordered ferromagnetic phase from the high-temperature paramagnetic one. The phase-diagram line separates the two phases of the model and intersects the randomness axis at the critical value of the disorder strength h_c, as shown in figure 1. Such qualitative sketching has been commonly used in most papers for the RFIM [22–27] and closed form quantitative expressions are also known from the early mean-field calculations [27].

Although nowadays the view that the phase transition of the RFIM is of second order, irrespective of the form of the random-field distribution and for all values of the disorder strength [28], there are still some puzzling behavior that remains contradictory. These refer mainly to the small value of the critical exponent β of the magnetization and, even more, to the scaling behavior of the specific heat and the corresponding value of the critical exponent α; the latter having severe implications for the modified hyperscaling relation [28–33].

In this paper we deal with the latter problem of the specific heat and we revisit its scaling behavior by recruiting powerful numerical and finite-size scaling techniques in order to obtain accurate numerical data through the extensive use of large simulation platforms. In particular we compute exact ground states of the model, as is explained shortly below.

The rest of the paper is laid out as follows: In Sec. 2 we present the general framework of the numerical method

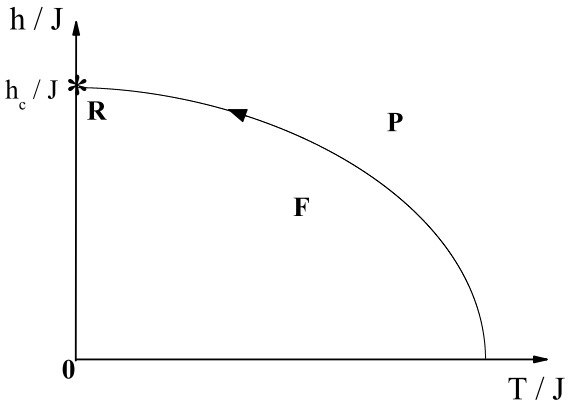

Fig. 1. Schematic phase diagram and renormalization-group flow of the RFIM. The solid line separates the ferromagnetic (**F**) and paramagnetic (**P**) phases. The black arrow shows the flow to the random fixed point (**R**) at zero temperature ($T = 0$) and $h = h_c$, as marked by the asterisk.

used, which is by today standard for the study of the RFIM and we also give the implemented random-field distribution. In Sec. 3 we define the specific-heat-like quantity under study and in Sec. 4 we present the finite-size scaling analysis of our numerical data. Our results for the critical exponent α are discussed under the prism of a modified Rushbrooke inequality for the case of a saturating specific heat. Our paper is concluded in Sec. 5 where a summary of the main results is given.

2 Simulation details

The calculation of the ground states is based on the mapping [36,34,35,37,28–33,38–50] to the maximum-flow problem [51–53]. This is a well-established combinatorial optimization problem which can be solved exactly using efficient, i.e., polynomial-time, optimization algorithms. A clear advantage of this approach is the ability to simulate large system sizes and disorder ensembles in rather moderate computational times. Here, we should underline that even the most efficient $T > 0$ Monte Carlo schemes exhibit extremely slow dynamics in the low-temperature phase of these systems and are upper bound by linear sizes of the order of $L_{\max} \leq 32$. Further asset in the $T = 0$ approach is the absence of statistical (sampling) errors, though the presence of statistical fluctuations coming from the disorder average is unavoidable. Additionally, the approach lacks equilibration problems, which are typical for Monte Carlo simulations, due to the fact that the ground states are exact. In this way we can omit the two major drawbacks encountered in the $T > 0$ simulation of systems with rough free-energy landscapes [14].

Note that the fact that we consider the model exactly at $T = 0$ is no restriction, since for this model it allows us to draw conclusions about the finite-temperature behavior, which is actually of interest: The random field is a relevant perturbation at the pure fixed point, which lies at $T = 0$ [14,17–20]. Hence, the critical behavior is the same everywhere along the phase boundary of figure 1, and we can predict it simply by staying at $T = 0$ and crossing the phase boundary at $h = h_c$.

The application of maximum-flow algorithms to the RFIM is nowadays well established [43]. The most efficient network flow algorithm used to solve the RFIM is the push-relabel algorithm of Tarjan and Goldberg [54]. For the interested reader, general proofs and theorems on the push-relabel algorithm can be found in standard textbooks [52,53]. The version of the algorithm implemented in our study involves a modification proposed by Middleton et al. [29,40,41] that removes the (technical) source and sink nodes, in this way reducing memory usage and also clarifying the physical connection [40,41].

For the disorder realizations as given by the random fields $\{h_i\}$ we used a Gaussian distribution of the form

$$\mathcal{P}(h_i) = \frac{1}{\sqrt{2\pi h^2}} \exp\left(-\frac{h_i^2}{2h^2}\right). \tag{2}$$

The main advantage of the above distribution (2) is that the ground state of the system is non-degenerate, so it is sufficient to calculate just one ground state in order to get the necessary information.

3 Specific heat

Our analysis concerns the controversial issue of the specific heat of the RFIM. The specific heat of the RFIM can be experimentally measured [15] and is of great theoretical importance. Yet, it is well known that it is one of the most intricate thermodynamic quantities to deal with in numerical simulations, even when it comes to pure systems. For the RFIM, Monte Carlo methods at $T > 0$ have been used to estimate the value of its critical exponent α, but were restricted to rather small systems sizes and have also revealed many serious problems, i.e., severe violations of self averaging [55,56]. A better picture emerged throughout the years from $T = 0$ computations, however, even by using the same numerical techniques, but different scaling approaches, some inconsistencies have been recorded in the literature. In particular, a wide range of estimates of α have been reported, from strongly negative values to values close to zero [28–33]. On the other hand, experiments on random field and diluted antiferromagnetic systems suggested a logarithmic divergence of the specific heat [15].

In the present work we employ a scaling approach on a specific-heat-like quantity as originally suggested by one of us (AKH) and Young [30], and we apply it to numerical data obtained for much larger system sizes compared to the original reference [30]. For more details on the derivation and similarities of the quantities of interest at positive and zero temperature we refer the reader to Section 2

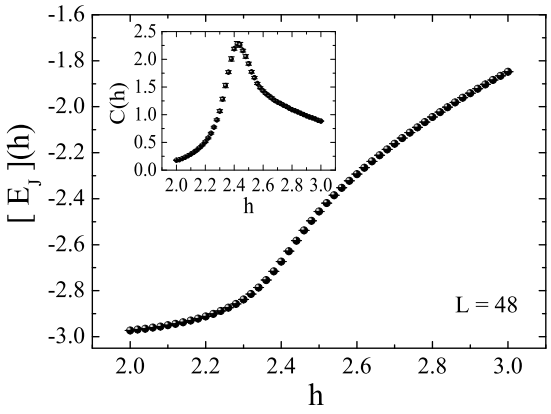

Fig. 2. The main figure shows the disorder-averaged bond energy $[E_J](h)$ per spin as a function of the random-field strength h for a system with linear size $L = 48$. The inset displays the resulting specific heat, calculated using the formula of equation (4).

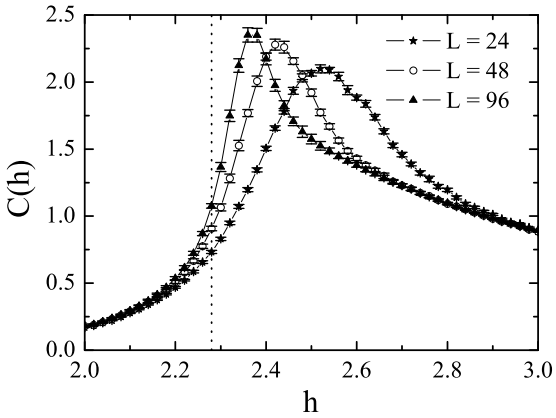

Fig. 3. A clear instance of the shift behavior of the specific heat C as a function of the random-field strength h for some typical systems sizes, as indicated in the figure. The solid lines are simple guides to the eye. The vertical dotted line indicates the location of the critical field strength, $h_c = 2.279$, as estimated below in figure 4.

of reference [30], where the full explanations and relevant scaling arguments are given.

A crucial point in this approach comes from the following observation: although in zero random field, the specific-heat exponent is obtained from the singularity in the second derivative of the free energy with respect to temperature, more generally it is determined from the singularity obtained by varying a parameter which crosses the phase boundary from the paramagnetic phase to the ferromagnetic phase. From figure 1 we see that this can be conveniently accomplished by keeping the ratio of h/J to T/J fixed, i.e., by varying J. Thus, according to reference [30], in order to observe the specific-heat singularity for the random-field case, the bond energy E_J is studied

$$E_J \equiv \frac{\partial F}{\partial J} = -\frac{1}{\mathcal{N}} \sum_{\langle i,j \rangle} \sigma_i \sigma_j, \tag{3}$$

where F denotes the free energy [57].

E_J has an energy-like singularity in the vicinity of the phase boundary. Having differentiated analytically with respect to J, we now set $J = 1$ and consider only $T = 0$. A specific-heat-like quantity is obtained by differentiating E_J numerically with respect to the random field h. A first-order finite difference is used to determine the derivative of E_J numerically and, since this is a more accurate representation of the derivative at the midpoint of the interval than at either endpoint, the specific heat, C, at $T = 0$ is defined to be

$$C\left(\frac{h_1 + h_2}{2}\right) \equiv \frac{[E_J(h_1)]_h - [E_J(h_2)]_h}{h_1 - h_2}, \tag{4}$$

where h_1 and h_2 are two close-by values of h. A sufficiently fine mesh of random-field values is chosen such that the resulting data for C is smooth.

4 Results and discussion

We performed large-scale zero-temperature simulations of the Gaussian RFIM for a wide range of the simulation parameters using the prescription of Sec. 2. In particular we considered random-field strengths $h \in [2.0-3.0]$ and linear sizes $L \in [4 - 268]$. Additionally, for each pair $(h,\ L)$ an extensive disorder averaging process has been undertaken, denoted as $[\cdots]$, by sampling over 50×10^3 independent random-field realizations for systems with $L \leq 200$ and 5×10^3 realizations for $L > 200$.

In the main panel of figure 2 the averaged over the disorder bond energy per spin $[E_J](h)$ is illustrated for a system size of $L = 48$. As expected, for very small values of h all spins point into the same direction and so $[E_J] \to -3$, whereas for large values h the spins follow the random fields and so, on average the number of satisfied and unsatisfied bonds are equal, hence $[E_J] \to 0$ in this limit. The inset of the same figure shows the corresponding specific heat, obtained as the numerical derivative of the data for $[E_J](h)$ according to equation (4). The specific heat is seen to have a clear peak at some pseudocritical value of h, denoted also as pseudocritical disorder strength h_L^*, and in what follows, we shall investigate the size dependence of this peak and the shift behavior of the pseudocritical fields h_L^*.

In a finite system, finite-size scaling predicts for the singular part C_s of the specific heat

$$C_s \sim L^{\alpha/\nu} \tilde{C}\left((h - h_c) L^{1/\nu}\right), \tag{5}$$

where ν is the correlation-length exponent. The specific-heat peak will occur when the argument of the scaling function $\tilde{C}$ takes some value, say a_1, so the peak position h_L^* varies as

$$h_L^* - h_c \approx a_1 L^{-1/\nu} \tag{6}$$

and the value of the singular part of the specific heat at the peak as

$$C_{\rm s}^{\rm max}(L) \sim L^{\alpha/\nu}. \quad (7)$$

For a more detailed description of the above scaling formulas we refer the reader to reference [30].

An alternative indirect route to the estimation of the critical exponent α, based again on the bond energy $[E_J]$, but this time at the supposedly known "exact" value of the critical field $h_{\rm c}$, may be found in references [29,31, 32]. The computation from the behavior of $[E_J]$ is based on integrating the above scaling equation (5) up to $h_{\rm c}$, which gives a dependence of the form $[E_J](L, h = h_{\rm c}) = k_1 + k_2 L^{(\alpha-1)/\nu}$ with k_i to be constants. Thus, assuming that we know the "exact" value of $h_{\rm c}$, one may fit the data of the bond energy $[E_J]$ to obtain the exponent ratio $(\alpha - 1)/\nu$ and then using an estimate of ν, calculate indirectly the critical exponent α of the specific heat. Obviously, as no a priori knowledge of the "exact" critical field value exists, what is usually done is to use some candidate values of $h_{\rm c}$ around the best known estimate and then repeat the simulations for all the candidate values. The first authors that actually implemented this method for the present model were Middleton and Fisher [29]. At their extensive study they obtained estimates for the exponent ratio $(\alpha-1)/\nu$ and quantified the error effects due to the uncertainty in the selection of the critical field value and to scaling corrections. Their original estimate of the critical exponent $\alpha = -0.12(12)$ from the scaling of the bond energy at the field value $h_{\rm c} = 2.27$ was then brought down to $\alpha = -0.01(9)$ by using a combined scheme that benefited further from some total stiffness measurements on isotropic and anisotropic systems with fixed boundary conditions. Following this work, the complementary analysis of reference [31] showed explicitly by large-scale simulations that indeed a change in the value of $h_{\rm c}$ by a factor of $\delta h_{\rm c} = 0.001$ results, on a average, in a change $\delta\alpha \approx 0.04$ in the value of α. In the current work we decided to analyze the specific-heat data directly, using the prescription of reference [30], in order to avoid these uncertainties but also to be able to test the various scaling scenarios that have been suggested in the extensive literature of the model. As a side target we are also interested in producing high-accuracy estimates of the critical field value and the critical exponent of the correlation length (see figure 4 below).

Figure 3 illustrates some characteristic numerical results for the specific heat of three selected system sizes as a function of the random field h. A clear peak can be seen, which moves to the left and increases in height with increasing system size. In our analysis, for each system size, we performed parabolic fits to the region of the peak to obtain the pseudocritical fields h_L^* and the height of the peaks $C^{\rm max}$. The shift of the maximum according to equation (6) can be used to estimate the infinite-size critical strength of the random field, $h_{\rm c}$ and the correlation-length exponent ν and this is shown in figure 4. The best fit, with a $\chi^2/{\rm DOF} = 0.9$, where DOF denotes the number of degrees of freedom, gives the values $h_{\rm c} = 2.279(7)$ and $\nu = 1.37(1)$ that compare very well to the most accurate estimations in the literature $h_{\rm c} = 2.27(1)$ and $\nu = 1.37(5)$ [28–33].

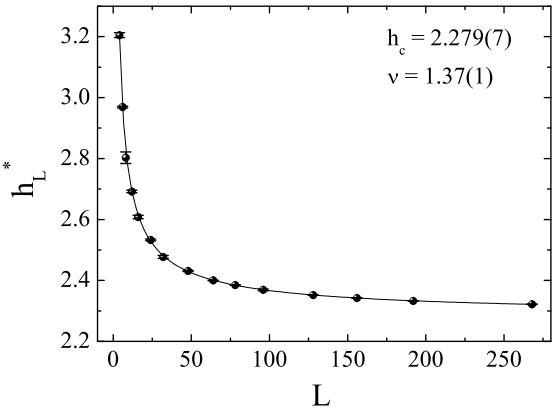

Fig. 4. Finite-size scaling behavior of the pseudocritical random fields h_L^*, i.e., of the fields where the specific heat attains its maximum, as a function of system size L. The solid line shows a fit to the function $h_L^* = h_{\rm c} + a_1 L^{-1/\nu}$ with $h_{\rm c} = 2.279(7)$, $a_1 = 2.56(4)$, and $\nu = 1.37(1)$.

Having simulated several lattice-size points, we also tried to perform the above fit including scaling corrections of the form $(1 + a_1' L^{-\omega})$, where ω is the well-known correction-to-scaling exponent, using it either as a free parameter or fixing it to the value $\omega = 0.52$, suggested recently in reference [28]. However, no improvement has been observed in the quality of the fit. On the contrary, the corrected scaling assumption resulted in an unstable fit procedure with significantly large errors in the values of the exponent ν and the coefficients a_1 and a_1'.

We now turn the discussion to the scaling behavior of the specific heat by investigating the evolution of $C^{\rm max}$ with the linear system size L. Our analysis and tests will be unfolded along the lines of the two main scenarios of the literature, that is a logarithmic divergence and the standard power-law behavior, including some small variations of these scaling laws.

If we assume $\alpha = 0$, then one expects a logarithmic divergence and the simplest hypothesis is to fit the data to

$$C^{\rm max}(L) = c_1 + c_2 \log(L), \quad (8)$$

where the constant term c_1 comes partly from the regular part of the specific heat. However, this scenario is not valid (see figure 5). A plot of $C^{\rm max}$ against L on a semi-log scale shows a clear curvature, suggesting that the height of the specific heat will saturate to a finite value as L increases. In particular, a fit to the scaling law (8) for $L \geq 12$ yields $c_1 = 1.53(12)$ and $c_2 = 0.18(3)$ with a $\chi^2/{\rm DOF} = 75$, indicating that the full data are not compatible with a logarithmic divergence. As a further test case, one may of course reduce the fit interval to make the data compatible to the logarithmic divergence. For instance, fitting over $L \geq 64$ one gets the values $c_1 = 2.08(4)$ and $c_2 = 0.071(8)$ with a $\chi^2/{\rm DOF} = 1.97$. But then, the small value of the

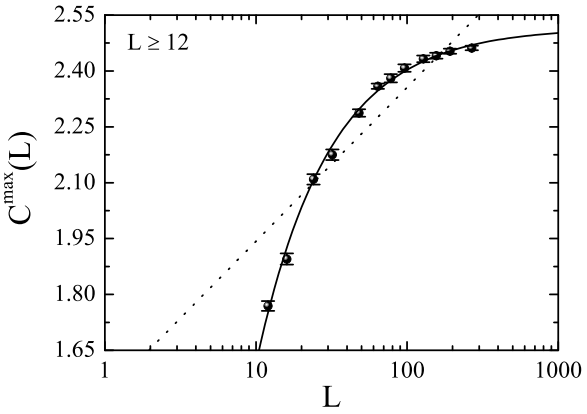

Fig. 5. Finite-size scaling of $C^{\max}$ with a logarithmic scale on the L-axis. The dotted and solid lines illustrate logarithmic (8) and power-law (10) fits respectively, for $L \geq 12$.

coefficient of the logarithm c_2 shows that the specific heat does not change significantly beyond $L = 64$, so one could probably fit almost every slightly increasing function. In fact, we performed tests that are omitted here for brevity and verified this assumption. Thus, one first important conclusion from the above analysis is that one should consider in the fits a lattice-size window which includes also smaller values of the linear size L, for instance the window $L = 12 - 268$ looks like a safe option.

As a variation of the simple logarithmic function, we also performed fits to a log (log) function, i.e., a very slow divergence of the form

$$C^{\max}(L) = n + o \log (p + q \log L). \tag{9}$$

The result of this fit over the window $L = 12-268$ yielded the following values for the coefficients (with huge error bars as it can be seen) $n = 2.28 \pm 6.10$, $o = 0.28 \pm 0.10$, $p = -1.4 \pm 29.1$, and $q = 0.62 \pm 13.19$ and a very bad quality of the fit $\chi^2/\mathrm{DOF} = 10.17$. Of course, our choice of the scaling law (9) is not necessarily relevant for the RFIM, as there are no calculations which predict this type of behavior for the model, but rather an example of a slowly diverging function, that according to the above results, is also excluded as well.

On the other hand now, taking into account the scenario of a peak height which saturates as $L \to \infty$, we tried a fit of the form

$$C^{\max}(L) = C_\infty + bL^x, \tag{10}$$

where x could be seen as an estimate for α/ν. When using again the sizes $L = 12-268$, this yielded the values $C_\infty = 2.52(1)$, $b = -7.20(9)$, and $x = -0.90(5)$, and a fit quality of $\chi^2/\mathrm{DOF} = 1.04$, indicating that the current data are compatible with a convergence of the specific heat to a constant, i.e., a cusp. If we restrict the scaling window to smaller system sizes of up to $L = 96$ for instance, the estimate of x is of the order of -0.5, compatible with the earlier result of reference [30].

Since C_∞ is about 200 standard deviations away from zero, we can safely argue that a pure power-law behavior is not compatible with the data. Furthermore, including a correction-to-scaling term of the standard form $(1+b'L^{-\omega})$ no improvement was observed also when we shifted the lattice-size window of the fit to larger values of L. Even more, as in the case of the scaling of the pseudocritical fields, large error bars appear, making the inclusion of the correction term meaningless also for this set of data. Thus, according to the above analysis, we may conclude that the numerical data of the specific heat are not compatible with a diverging behavior but seem to be well described by a convergence to a constant.

Now, we discuss the relevance of the above results for the specific heat with respect to the standard scaling relations. In particular, we consider the Rushbrooke inequality

$$\alpha + 2\beta + \gamma \geq 2. \tag{11}$$

Clearly, using the established values $\gamma = 2.05(5)$ [28] and $\beta = 0.017(5)$ [29], the inequality (11) is not fulfilled when using a strongly negative value of $\alpha = x\nu = -1.23(7)$ since one obtains $\alpha + 2\beta + \gamma = 0.85(9) \ll 2$. This apparent violation of the scaling relation has in fact been reported as one of the main controversial issues in the study of the RFIM [58]. To our knowledge, equation (11) holds in all other models and emerges from well-known scaling theories and the renormalization group. In these approaches the scaling of the singular part of the free energy is considered, and so this result is expected to hold even if α is (strongly) negative. Therefore, we may expect that there must be some subtlety associated with this being a zero-temperature fixed point, or with the definition of the energy as a J-derivative, which invalidates the exponent relation. We know that the zero-temperature nature of the fixed point does affect hyperscaling relations, but up to now, it is accepted that those exponent relations not involving D should be valid for the RFIM unmodified. This remains as an open question for the random-field problem. We should note here that the numerical works [29,32], where the scaling of the bond energy is studied at the critical point, get α also negative but close to zero and hence almost consistent with the Rushbrooke relation within error bars. In particular, Theodorakis and Fytas [32] performed simulations for system sizes up to $L = 156$ at the proposed in reference [28] critical-field estimate $h_c = 2.227205$. Their finite-size scaling analysis of the bond energy suggested an estimate $\alpha = -0.095(37)$, for the critical exponent of the specific heat. This value is indeed very close to zero and also compatible to the value $\alpha = -0.12(12)$ of Middleton and Fisher [29], obtained by a similar analysis but from simulations performed at a different candidate critical value, namely the value $h_c = 2.27$, as also discussed above.

Motivated by the above controversy with respect to the Rushbrooke inequality, we have reconsidered its original derivation for the case of a saturating specific heat, simply by going one step back in the calculation. Of course our discussion below refers to the standard specific-heat definition at constant field, but we believe that the reasoning outlined is also meaningful for the present case, via the

described in reference [29] analogy of the specific-heat definitions at positive and zero temperature. Equation (11) stems from the fundamental Maxwell relation

$$\chi(C - C_m) = T \left(\frac{\partial m}{\partial T} \right)^2 , \tag{12}$$

with m being the magnetization, C_m the heat capacity at constant magnetization and χ the susceptibility. Using the fact that C, C_m, and χ are all larger than zero, one obtains

$$C \geq \frac{T}{\chi} \left(\frac{\partial m}{\partial T} \right)^2 . \tag{13}$$

When assuming, for $t < 0$ being the distance to the critical point in the ordered phase, power-law behavior $C \sim (-t)^{-\alpha}$, $\chi \sim (-t)^{-\gamma}$, and $m \sim (-t)^{\beta}$, by taking the logarithm and dividing by $\ln(-t) \to -\infty$ for $t \to 0^-$, one arrives at (11), since any prefactor in (13) will drop out. Clearly, equation (13) involves the complete formula of the thermodynamic specific heat, not only non-analytic terms. Thus, if the specific heat is given by a cusp, i.e., a power-law convergence to a constant according to $C = C_\infty + b(-t)^{-\alpha}$, this full form must inserted into equation (13). Now, by taking the logarithm and dividing by $\ln(-t)$ the left side will become zero, thus one is left with $2\beta + \gamma \geq 2$. This corresponds to an effective value $\tilde{\alpha} = 0$, i.e., describing a constant when approaching the critical point, for the specific heat if one still likes to write $\tilde{\alpha} + 2\beta + \gamma \geq 2$. This latter relation is fulfilled now, even as an equality within error bars using the most accurate values of γ and β mentioned above. Thus, we may conclude that when describing the approach to the constant one is still free to state the exponent $\alpha < 0$ but when it comes to the Rushbrooke inequality the value of $\tilde{\alpha} = 0$ seems more reasonable to use.

5 Conclusions

To summarize, in the present paper we revisited the scaling of the specific heat of the three-dimensional Gaussian random-field Ising model. Numerically, the present work became feasible via the mapping of the model into a network and obtaining the maximum flow through a modified version of the push-relabel algorithm. Due to the polynomial running time of the algorithm, this scheme enabled us to simulate for a wide range of the random-field strength h systems of up to 268^3 spins, averaging for each pair $(h,\ L)$ over several thousands of independent random realizations. Following the approach of reference [30], by numerically differentiating the bond energy with respect to h, a specific-heat-like quantity was obtained whose finite-size scaling was found to be compatible with a convergence, via $\alpha/\nu = -0.90(5)$, to a constant. This strongly negative value of α clearly invalidates the Rushbrooke inequality and it is still not clear to us if this is relevant to the nature of the zero-temperature fixed point or if it is related to the definition of the specific-heat-like quantity studied. Given that many large-scale numerical works, including ours, have not succeeded in providing concrete answers to this question, this problem remains open and calls for a better theoretical understanding. However, motivated by this apparent and non-settled controversy in the random-field problem, we have worked out the implications of a constant specific heat at the thermodynamic limit with respect to the derivation of the Rushbrooke inequality via the Maxwell construction that involves the complete scaling form of the specific heat, including the constant term C_∞. For this particular case, the inequality $2\beta + \gamma \geq 2$ seems to be more reasonable to use. Finally, the extensive simulations performed allowed us to provide high-accuracy estimates of the critical field $h_c = 2.279(7)$ and the critical exponent of the correlation exponent $\nu = 1.37(1)$ that compare very well to the current literature of the model.

The authors would like to thank Prof. A.P. Young for useful discussions. Part of the simulations were performed at the HERO cluster of the University of Oldenburg, jointly funded by the DFG (INST 184/108-1 FUGG) and the ministry of Science and Culture (MWK) of the Lower Saxony State. N.G. Fytas acknowledges financial support from a Royal Society Research Grant under No RG140201.

All authors contributed equally to this work.

References

1. Y. Imry and S.-K. Ma, Phys. Rev. Lett. **35**, 1399 (1975).
2. A. Aharony, Y. Imry, and S.-K. Ma, Phys. Rev. Lett. **37**, 1364 (1976).
3. A.P. Young, J. Phys. Condens. Matter **10**, L257 (1977).
4. S. Fishman and A. Aharony, J. Phys. Condens. Matter **12**, L729 (1979).
5. G. Parisi and N. Sourlas, Phys. Rev. Lett. **43**, 744 (1979).
6. J.L. Cardy, Phys. Rev. B **29**, 505 (1984).
7. J.Z. Imbrie, Phys. Rev. Lett. **53**, 1747 (1984).
8. M. Schwartz and A. Soffer, Phys. Rev. Lett. **55**, 2499 (1985); Phys. Rev. B **33**, 2059 (1986); M. Schwartz, J. Phys. Condens. Matter **18**, 135 (1985); M. Schwartz, M. Gofman, and T. Nattermann, Physica A **178**, 6 (1991); M. Schwartz, Europhys. Lett. **15**, 777 (1994).
9. M. Gofman, J. Adler, A. Aharony, A.B. Harris, and M. Schwartz, Phys. Rev. Lett. **71**, 1569 (1993).
10. J. Esser and U. Nowak, Phys. Rev. B **55**, 5866 (1997).
11. W.C. Barber and D.P. Belanger, J. Magn. Magn. Mater. **226**, 545 (2001).
12. D.P. Belanger and A.P. Young, J. Magn. Magn. Mater. **100**, 272 (1991).
13. H. Rieger, in *Annual Reviews of Computational Physics II* (ed. D. Stauffer), 295-341, World Scientific, Singapore 1995.
14. See, e.g., the articles by D.P. Belanger and T. Nattermann in *Spin Glasses and Random Fields*, A.P. Young (Ed.), World Scientific, 1998.
15. D.P. Belanger, A.R. King, V. Jaccarino, and J.L. Cardy, Phys. Rev. B **28**, 2522 (1983); D.P. Belanger and Z. Slanič, J. Magn. Magn. Mater. **186**, 65 (1998).
16. R.L.C. Vink, K. Binder, and H. Löwen, Phys. Rev. Lett. **97**, 230603 (2006).
17. J. Villain, Phys. Rev. Lett. **52**, 1543 (1984); J. Physique **46**, 1843 (1985).

18. A.J. Bray and M.A. Moore, J. Phys. Condens. Matter **18**, L927 (1985).
19. D.S Fisher, Phys. Rev. Lett. **56**, 416 (1986).
20. A.N. Berker and S.R. McKay, Phys. Rev. B **33**, 4712 (1986).
21. J. Bricmont and A. Kupiainen, Phys. Rev. Lett. **59**, 1829 (1987).
22. M.E.J. Newman, B.W. Roberts, G.T. Barkema, and J.P. Sethna, Phys. Rev. B **48**, 16533 (1993).
23. J. Machta, M.E.J. Newman, and L.B. Chayes, Phys. Rev. E **62**, 8782 (2000).
24. M.E.J. Newman and G.T. Barkema, Phys. Rev. E **53**, 393 (1996).
25. M. Itakura, Phys. Rev. B **64**, 012415 (2001).
26. N.G. Fytas and A. Malakis, Eur. Phys. J. B **61**, 111 (2008).
27. A. Aharony, Phys. Rev. B **18**, 3318 (1978); A. Aharony, Phys. Rev. B **18**, 3328 (1978); T. Schneider and E. Pytte, Phys. Rev. B **15**, 1519 (1977); D. Andelman, Phys. Rev. B **27**, 3079 (1983).
28. N.G. Fytas and V. Martín-Mayor, Phys. Rev. Lett. **110**, 227201 (2013).
29. A.A. Middleton and D.S. Fisher, Phys. Rev. B **65**, 134411 (2002).
30. A.K. Hartmann and A.P. Young, Phys. Rev. B **64**, 180404 (2001).
31. P.E. Theodorakis, I. Georgiou, and N.G. Fytas, Phys. Rev. E **87**, 032119 (2013).
32. P.E. Theodorakis and N.G. Fytas, Condens. Matter Phys. **17**, 43003 (2014).
33. N.G. Fytas, P.E. Theodorakis, I. Georgiou, and I. Lelidis, Eur. Phys. J. B **86**, 268 (2013).
34. A.K. Hartmann and K.D. Usadel, Physica A **214**, 141 (1995); A.K. Hartmann, Physica A **248**, 1 (1998).
35. S. Bastea and P.M. Duxbury, Phys. Rev. E **58**, 4261 (1998); S. Bastea, Phys. Rev. E **58**, 7978 (1998); S. Bastea and P.M. Duxbury, Phys. Rev. E **60**, 4941 (1999).
36. A.T. Ogielski, Phys. Rev. Lett. **57**, 1251 (1986).
37. A.K. Hartmann and U. Nowak, Eur. Phys. J. B **7**, 105 (1999).
38. A.K. Hartmann, Phys. Rev. B **65**, 174427 (2002).
39. E.T. Seppälä and M. J. Alava, Phys. Rev. E **63**, 066109 (2001) ; E.T. Seppälä, M.J. Alava, and P.M. Duxbury, Phys. Rev. E **63**, 066110 (2001); E.T. Seppälä, A.M. Pulkkinen, and M.J. Alava, Phys. Rev. B **66**, 144403 (2002).
40. A.A. Middleton, Phys. Rev. Lett. **88**, 017202 (2002).
41. A.A. Middleton, arXiv:cond-mat/0208182; J.H. Meinke, A.A. Middleton, arXiv:cond-mat/0502471; D.C. Hambrick, J.H. Meinke, A.A. Middleton, arXiv:cond-mat/0501269.
42. I. Dukovski and J. Machta, Phys. Rev. B **67**, 014413 (2003).
43. M.J. Alava, P.M. Duxbury, C.F. Moukarzel, and H. Rieger, in *Phase Transitions and Critical Phenomena*, Vol. 18, edited by C. Domb, J.L. Lebowitz, (Academic Press, San Diego, 2001).
44. M. Zumsande, M.J. Alava, and A.K. Hartmann, J. Stat. Mech.: Theory Exp. (2008) P02012.
45. G.P. Shrivastav, S. Krishnamoorthy, V. Banerjee, and S. Puri, Europhys. Lett. **96**, 36003 (2011).
46. B. Ahrens and A.K. Hartmann, Phys. Rev. B **83**, 014205 (2011); Phys. Rev. B **84**, 144202 (2011); Phys. Rev. B **85**, 224421 (2012).
47. J.D. Stevenson and M. Weigel, Europhys. Lett. **95**, 40001 (2011); Comput. Phys. Commun. **182**, 1879 (2011).
48. N.G. Fytas, P.E. Theodorakis, and I. Georgiou, Eur. Phys. J. B **85**, 349 (2012).
49. A.K. Hartmann and H. Rieger, *Optimization Algorithms in Physics*, (Wiley-VCH, Berlin 2004).
50. A.K. Hartmann and M. Weigt, *Phase Transitions in Combinatorial Optimization Problems*, (Wiley-VCH, Berlin 2005).
51. J.-C. Anglés d Auriac, M. Preissmann, and R. Rammal, J. Phys. Lett. **46**, L173, (1985).
52. T.H. Cormen, C.E. Leiserson, and R.L. Rivest, *Introduction To Algorithms*, (MIT Press, Cambridge, MA, 1990).
53. C.H. Papadimitriou, *Computational Complexity*, (Addison-Wesley, Reading, MA, 1994).
54. A.V. Goldberg and R.E. Tarjan, J. Assoc. Comput. Mach. **35**, 921 (1988); B.V. Cherkassky and A.V. Goldberg, Algorithmica **19**, 390 (1997).
55. G. Parisi and N. Sourlas, Phys. Rev. Lett. **89**, 257204 (2002); G. Parisi, M. Picco, and N. Sourlas, Europhys. Lett. **66** 465 (2004).
56. A. Malakis and N.G. Fytas, Phys. Rev. E **73**, 016109 (2006).
57. Note that the role taken by the free energy at finite temperature is played by the energy at $T = 0$, since the two are equal in this limit according to the relation $F = E - TS$.
58. U. Nowak, K.D. Usadel, and J.Esser, Physica A **250**, 1 (1998).